PREDICTION OF PEAK GROUND ACCELERATION OF SHALLOW CRUSTAL EARTHQUAKES USING DEEP NEURON NETWORK

D. Ji[(1)], W. Wen[(2)], C. Zhai[(3)] , C. Li[(4)]

[(1)] *Assistant Professor, School of Civil Engineering, Harbin Institute of Technology, Harbin, China, jiduofa@hit.edu.cn*
[(2)] *Assistant Professor, School of Civil Engineering, Harbin Institute of Technology, Harbin, China, wenweiping@hit.edu.cn*
[(3)] *Professor, School of Civil Engineering, Harbin Institute of Technology, Harbin, China, zch-hit@hit.edu.cn*
[(4)] *PhD Candidate, School of Civil Engineering, Harbin Institute of Technology, Harbin, China, 19b933058@stu.hit.edu.cn*

Abstract

Ground motion prediction equations (GMPEs) can provide estimates of peak ground motion parameters (e.g., PGA,) by considering the effects of earthquake magnitude, distance, site, and source, which is a crucial element in the seismic hazard analysis. These equations help to evaluate the mean/median ground shaking effects for the expected levels of earthquakes. Thus, many empirical GMPEs were developed based on regression analysis, but they are highly uncertain due to the uncertainties of independent variables. To overcome this issue, the artificial neural network (ANN) is applied in the field of seismology and earthquake engineering to predict ground motion intensity measures (IMs). However, even though the ANN can produce high prediction accuracy, the defects are apparent, such as the database is relatively small. As a result, a challenging problem that arises in this domain is whether an artificial intelligence-based method can predict the attenuation relationship of ground motion parameters as well as response spectra based on a big database, which has not been reported elsewhere. Recently, deep neural network (DNN) has received much attention from engineering and is playing a crucial role in providing big data predictive models. Therefore, this study develops a DNN trained by the recordings from the PEER NGA-West2 database to predict peak ground motion acceleration (PGA). To this end, we collect 20,900 GMs based on the proposed criteria from the PEER NGA-West2 database and randomly split them into the training, validation, and testing datasets. The developed model relates PGA to earthquake source to site distance, earthquake magnitude, average shear-wave velocity, faulting mechanisms, and focal depth. The prediction errors are evaluated by three performance indicators, and the predictive results are compared with five well-known empirical models and one artificial neuron network model developed based on the PEER NGA-West2 database. The between-event and within-event residuals are calculated and compared with other models. Based on the results, our model has the best goodness-of-fit statistics of all the GMPEs we have compared, confirming that the proposed model is associated with better predictive power.

Keywords: ground motion, PGA, ground motion prediction model, deep neuron network

1. Introduction

Ground motion prediction equations (GMPEs) can provide estimates of peak ground motion parameters (e.g., PGA,) by considering the effects of earthquake magnitude, distance, site, and source, which is a crucial element in the seismic hazard analysis. These equations help to evaluate the mean/median ground shaking effects for the expected levels of earthquakes. Therefore, scholars are devoting to developing GMPEs based on local, regional, or global strong ground motion databases. For example, Esteva and Rosenblueth [1] proposed the first ground motion prediction model (GMPM) in which earthquake magnitude and distance are included. The proposed model was developed based on the least-squares regression of 46 earthquake records, and it can be used to estimate peak ground acceleration (PGA). Similarly, the first GMPM for response spectra was derived by Johnson [2] who developed an empirical model based on 23 earthquake records. The proposed equations can be used to predict the earthquake pseudo-relative velocity response spectra (PSRV) for a given earthquake magnitude and epicentral distance.

In 2003, the Pacific Earthquake Engineering Research Center (PEER) launched a large project (called NGA-West1) [3] that aims to develop next-generation GMPEs for shallow crustal earthquakes in active tectonic regions. A strong ground motion database [4] and five GMPEs [5–9] were announced as research

results of the project. The latter receives much attention throughout the world and is widely applied to research and engineering. However, some problems of GMPEs were exposed over time, such as poor prediction accuracy for earthquakes with small magnitude. Therefore, another program [10], called NGA-West2, was initiated, and a new strong ground motion database [11] and five GMPEs [12–16] were published in 2014. For example, Boore et al. [13] proposed GMPEs (hereafter called BSSA14) for PGA, PGV, and 5% damped PSA for moment magnitude from 3.0 to 7.9 earthquake events in NGA-West2 and a significant improvement was found when comparing with the GMPEs [17] proposed based on NGA-West1.

There are also many specific GMPEs for local area or countries, such as California [18], Canada [19], Eastern North America [20,21], Europe [22,23], Italy [24,25], Japan [26,27], New Zealand [28], and China [29,30]. For some regions (e.g., California, Europe, Italy, Japan, China) with sufficient ground motions, an empirical GMPE can be derived by using past earthquake records. For example, Chiou et al. [18] selected data from the California ShakeMap systems and developed a GMPE in which small-to-moderate shallow crustal earthquakes are considered. For some regions (e.g., eastern North America) with insufficient ground motions, a stochastic simulation method, called hybrid empirical method [21], was proposed and used to develop a GMPE. The results showed that the hybrid empirical method could provide a good prediction accuracy. However, the majority of existing GMPEs are derived based on empirical regression analysis of recorded strong ground motions. However, coefficients of the independent variables in GMPEs are significantly affected by the high nonlinearity and inhomogeneity among the independent variables. Moreover, the regression equation is derived on the basis of a predefined linear or nonlinear equation, with the assumption of the normal distribution of residuals for testing the developed equation. Hence, the GMPEs based on regression analysis are highly uncertain as a result of computational uncertainties and the uncertainties of independent variables [31].

Recently, many new techniques (e.g., artificial intelligence and soft computing) have been applied in civil/earthquake engineering and attracted a lot of attention [32–35]. Along these lines, many researchers took advantage of these new techniques to model ground motion parameters and response spectra. For example, Derras et al. [36] proposed a GMPE for PGA based on the KiK-net data using the artificial neural network (ANN), and they concluded that ANN is less sensitive to the dataset than classical methods (i.e., least-squares) that were used to obtain empirical GMPEs. After that, ANN has been widely applied in the field of seismology and earthquake engineering to predict ground motion intensity measures (IMs). More recently, Derras et al. [37] investigated the effect of site-condition proxies on the aleatory variability of GMPEs by using an ANN approach based on a total of 1028 recording from the PEER NGA-West2 database. A prediction equation was developed and the results were compared with BSSA14 to illustrate its performance. As presented above, even though the soft computing methods can produce high prediction accuracy, the defects are apparent, such as the database is relatively small. As a result, a challenging problem that arises in this domain is whether an artificial intelligence-based method can predict the attenuation relationship of ground motion parameters as well as response spectra based on a big database, which has not been reported elsewhere. Nowadays, deep neural network (DNN) is receiving much attention from engineering (e.g., [38–43]) and is playing a crucial role in developing big data predictive models [44,45]. Therefore, one possible way to solve the problem is by using DNN.

To this end, this paper aims to develop a predictive model for PGA based on the PEER NGA-West2 database by DNN. First, a total of 20,900 GMs are collected based on the proposed criteria from the PEER NGA-West2 database. Then, DNN is adopted to develop the predictive model for the PGA based on the collected GMs of which 80%, 10%, and 10% are randomly split into the training, validation, and testing datasets, respectively. The performance of the three datasets is assessed by three indicators that are widely used in previous investigations. Finally, the predictive power of the DNN model is verified by comparing its prediction results with those predicted by the four empirical models as well as an ANN model, and by systematically evaluating the between-event residuals and within-event residuals.

2. Database and performance indicators

2.1. Database

The GM database used herein was built based on the PEER NGA-West2 database [11] which is the newest database for shallow crustal earthquakes in active tectonic regions. The following criteria are used to build a subset of the PEER NGA-West2 database:

(1) records having two horizontal components;
(2) stations with the measured value of V_{S30};
(3) earthquakes with the information of magnitude, distance, and site metadata;
(4) excluding non-free field conditions and low-quality data;
(5) excluding recordings from earthquakes originating in oceanic crust; and
(6) excluding earthquakes which have less than four recordings;

It should be noted that this study used the RotD50 [46] version of the NGA-West2 flatfile [11] where the values of PGA, as well as source, site, and path information adopted herein, can be found. Finally, a total of 20,900 GM recordings were collected from 429 earthquakes with moment magnitude **M** ranging from 3 to 8 and R_{JB} ranging from 0 to 1600 km. Figure 1 illustrates the distribution of magnitude-distance and magnitude-soil condition pairs for the selected GMs in this study, respectively.
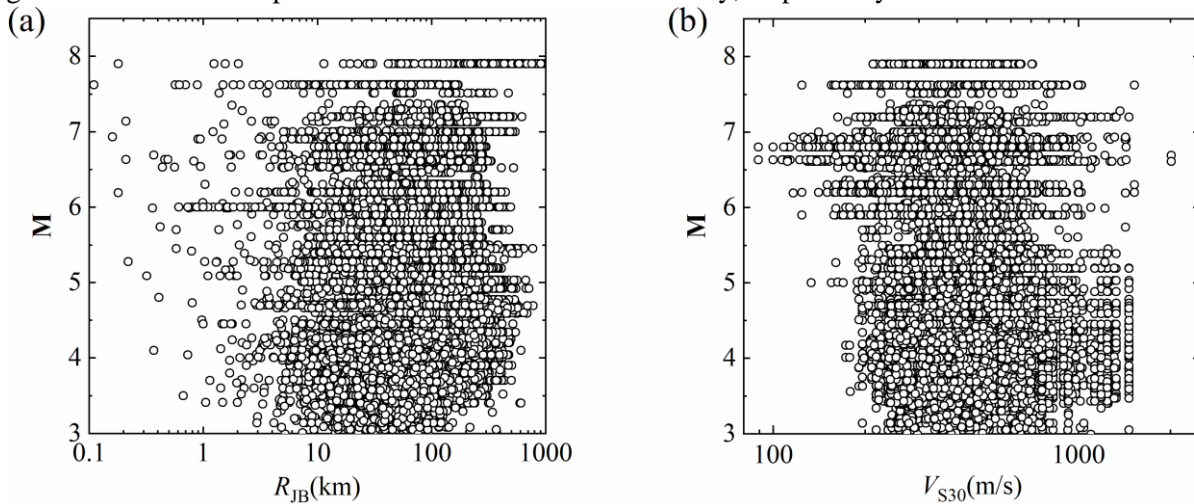
Fig. 1. Distribution of magnitude-distance and magnitude-soil condition pairs for the GMs from the PEER NGA-West2 database: (a) magnitude-distance pair; (b) magnitude-soil condition pair.

2.2. Performance indicators

To evaluate the prediction accuracy, the correlation coefficient, R, was first calculated, as it can measure the degree of linear dependence between the observed and predicted values. The correlation coefficient, R, can be mathematically expressed as follows:

$$R = \frac{\sum_{i=1}^{n}\left(y_i - \bar{y}\right)\left(y_i^{\text{pre}} - \bar{y}^{\text{pre}}\right)}{\sqrt{\sum_{i=1}^{n}\left(y_i - \bar{y}\right)^2 \sum_{i=1}^{n}\left(y_i^{\text{pre}} - \bar{y}^{\text{pre}}\right)^2}} \tag{1}$$

where y is the total amount of data, $\bar{y}$ is the mean observed value, $\bar{y}^{\text{pre}}$ is the mean predicted value.

The value of R equal to 0 means that there is no linear relationship between the observed and predicted values, while the value of R equal to 1 indicates that a linear relationship exists between the observed and predicted value. The defects of the correlation coefficient, R, are also evident, although it can effectively reflect the degree of linear dependence between the observed and the predicted values. For example, R is found to be insensitive to the amplitude changes of the predicted values, particularly in the scenario that y_i^{pre} are multiplied by a constant. Thus, two additional indicators (i.e., mean square error, mean absolute error) were computed to evaluate the prediction accuracy. The mathematical expressions of these two indicators can be written as follows:

3

$$MSE = \frac{1}{n}\sum\nolimits_{i=1}^{n}\left(y_i - y_i^{pre}\right)^2 \tag{2}$$

$$MAE = \frac{1}{n}\sum\nolimits_{i=1}^{n}\left|y_i - y_i^{pre}\right| \tag{3}$$

where MSE represents mean square error, MAE represents mean absolute error.

3. Comparison of the DNN model with the GMPEs model

The distribution of observed PGA values versus predicted ones using the DNN model are shown in Figure 2 for the training, validation, and testing datasets, respectively. The similarity in the scattered data distribution for the three datasets indicates a very similar degree of predictive power (i.e., *R* in Table 1) for the datasets, which means that the DNN model achieves a reliable prediction. To check whether the trained neural network is overfitted or not, the MSE and MAE are calculated for the training, validation and testing datasets respectively, as shown in Table 1.
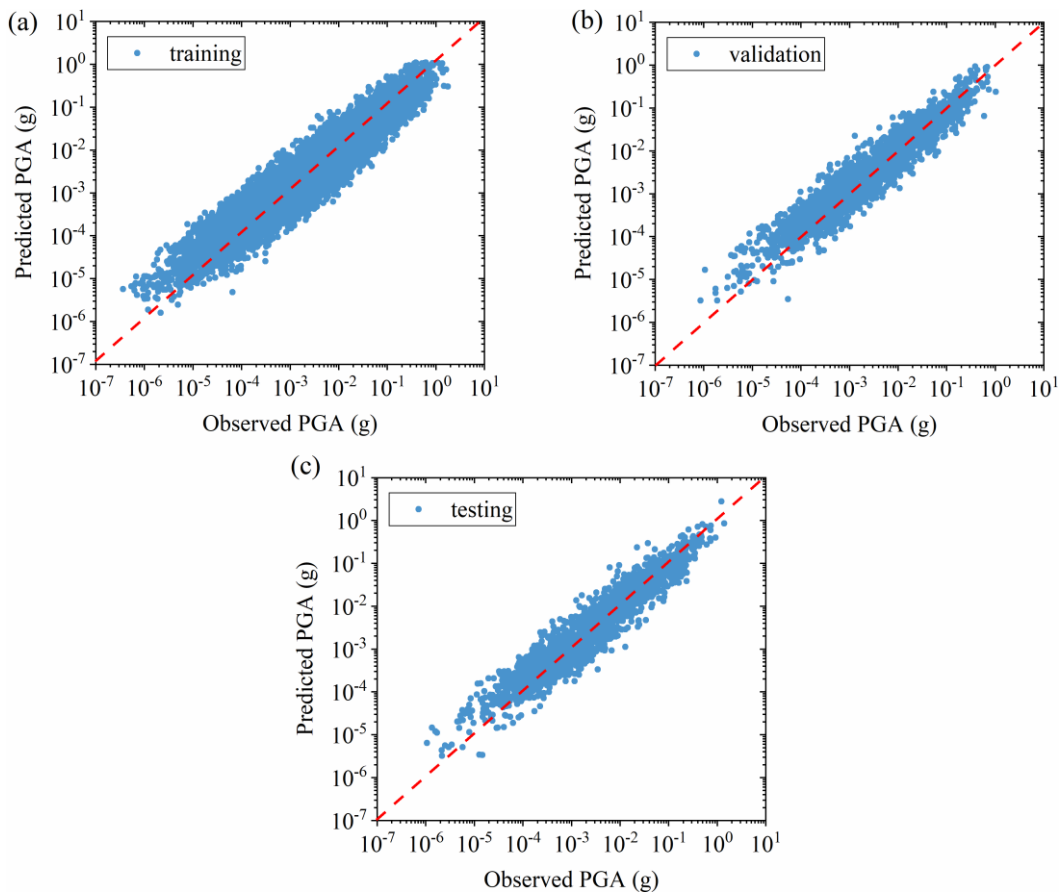
Fig. 2. Distribution of observed and predicted PGA values for DNN model using the GMs from the PEER NGA-West2: (a) training datasets; (b) validation datasets; (c) testing datasets.

Table 1. Comparison of the training, validation, and testing datasets with different performance indicators.

Datasets	*R*	MSE	MAE
Training	0.9566	0.0019	0.0124
Validation	0.9555	0.0017	0.0122
Testing	0.9639	0.0025	0.0126

To verify the validity of the DNN model, the predicted results by the DNN model were compared with

those by other GMPEs. There are many available GMPEs in literature, and however, for a fair comparison, we only selected the GMPEs proposed based on the PEER NGA-West2 database. Thus, a comparison of the proposed DNN model and four well-known GMPEs (i.e., hereafter called ASK14 [12], BSSA14 [13], CB14 [14], CY14 [15] are presented in Figure 3. Besides, an additional model developed by the ANN approach was also selected as a comparison pair (hereafter called ANN [37]). The performance indicators of PGA were listed in Table 2.
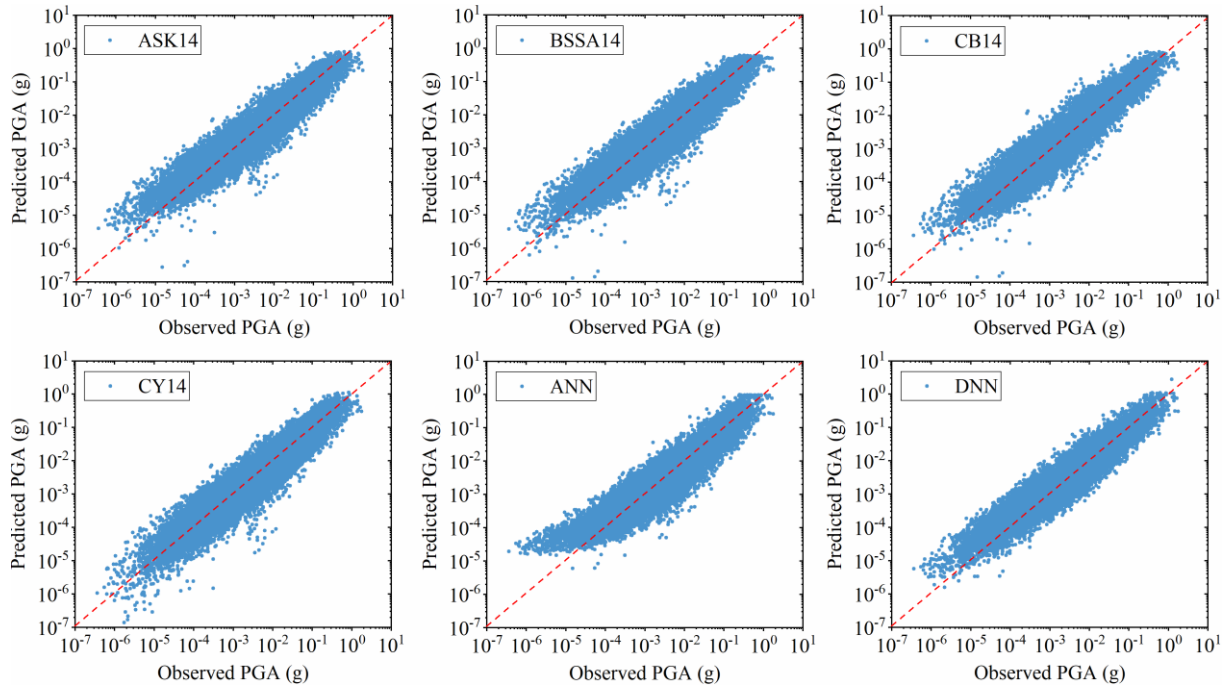
Fig. 3. Distribution of observed and predicted PGA values by six prediction models using the GMs from the PEER NGA-West2.

Table 2. Comparison of the predicted results of the six models for the NGA-West2 with different performance indicators.

Models	R	MSE	MAE
ASK14	0.9464	0.0020	0.0129
BSSA14	0.9439	0.0020	0.0133
CB14	0.9468	0.0019	0.0130
CY14	0.9467	0.0021	0.0133
ANN	0.9379	0.0024	0.0141
DNN	0.9562	0.0019	0.0125

It can be observed from Figure 2 that the DNN model gives better precision as the predicted PGA values are closer to the observed ones, compared to other models. The prediction accuracy is also corroborated by Table 2 as the DNN model has the highest R values. According to a rational hypothesis, it shows a strong correlation between the predicted and observed values when a model has a value of correlation coefficient, R, higher than 0.8. Thus, the four empirical GMPEs and the ANN model also achieve a high degree of predictive accuracy. Furthermore, the DNN model also presents the lowest errors (i.e., MSE and MAE). Therefore, the DNN model demonstrates a better prediction ability even though the five models have shown a good prediction performance.

4. Prediction results and residuals

4.1. Prediction results

5

For simplicity, the predicted results for the DNN model are only compared to those for the BSSA14 model in Figure 4 for a strike-slip scenario at a V_{S30} value of 760 m/s varying with **M** and R_{JB}, respectively. It is shown in Figure 4 that pronounced **M**-scaling of PGA can be observed for **M**<6. The amplitude-saturation can be seen from the distance attenuation trends that amplitudes are nearly constant in short-distance regions. Besides, ground motions with smaller magnitudes will attenuate more rapidly with distance than those with large magnitudes due to duration and finite-fault effects. The PGA values for the DNN model show a consistent trend with those for the BSSA14 model at short distances, while the differences between the two models become visible with the distance increases.
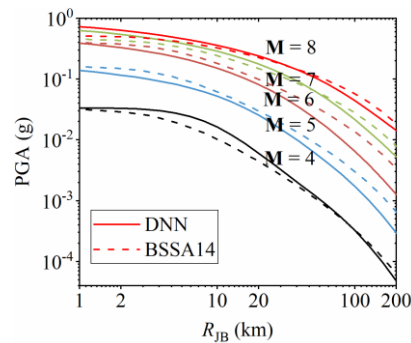
Fig.4. Comparison of the PGA from the DNN model with the median from the BSSA14 model for strike-slip earthquakes and $V_{S30} = 760$ m/s.

4.2. Between-event and within-event residuals

The analysis of residuals is a common way to evaluate the performance of predictive models because the residuals can reflect the relative predictive error of models. The residuals are usually separated into between-event and within-event terms by using the random-effects method [47], as follows:

$$\ln\left(IM_{GM}\right)_{ij} = \overline{\ln\left(IM_{GM}\right)_{ij}} + \eta_i + \varepsilon_{ij} \tag{4}$$

where $\ln\left(IM_{GM}\right)_{ij}$ and $\overline{\ln\left(IM_{GM}\right)_{ij}}$ are the observed and predicted logarithmic IM_{GM} value for the *i*-th event and *j*-th GM, respectively, η_i is the between-event residual, ε_{ij} is the within-event residual.

To assess the validity of the DNN model, Figure 5 plots the distribution of between-event residuals with respect to moment magnitude. Figure 6 shows the within-event residuals with respect to R_{JB} for PGA. Note that a positive residual means the DNN model underestimates the recording, while a negative residual means that the DNN model overestimates the recordings. From these plots, no significant bias or trend between residuals and predictor variables included in the DNN model can be observed. In general, these residual plots clearly indicate that the DNN model is robust and reliable.
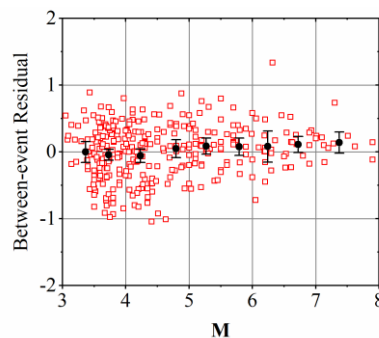
Fig. 5. Distribution of between-event residuals for PGA with respect to moment magnitude (M). Error bars represent the mean and 95th-percentile confidence limits of the mean binned residuals.

6
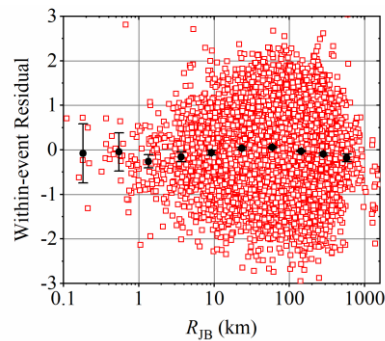
Fig. 6. Distribution of within-event residuals for PGA with respect to distance (R_{JB}). Error bars represent the mean and 95th-percentile confidence limits of the mean binned residuals.

5. Conclusions

The aim of the study is to develop GM predictive models for the PGA based on the PEER NGA-West2 database. A total of 20,900 earthquake records from 429 global shallow crustal earthquake events with **M** 3–8 and R_{JB} 0–1600 km were collected to build the database where 80%, 10%, and 10% of the database were randomly split into the training, validation, and testing datasets. Four empirical models and one ANN model were selected as comparison pairs. Deep neural network (DNN) was carefully designed, and the validity of the DNN model was verified by systematically comparing with the other prediction models. The residuals and standard deviations were systemically investigated. Some findings are listed as follows:

1. Irrespective of the training, validation, and testing datasets, high values of correlation coefficient and low values of MSE and MAE were found for the DNN model, indicating that the DNN model is a robust and reliable tool which is insensitive to the dataset.
2. Selected empirical models and an ANN model present a good performance for the PEER NGA-West2 database, while relatively better performance could be found for the DNN model.
3. The performance of the DNN model is on par with the BSSA14 model for large magnitudes, while the apparent difference for two models can be found for small magnitudes.
4. No significant bias or trend between residuals and predictor variables included in the DNN model can be observed.

6. Acknowledgments

7. References

[1] 2Esteva L, Rosenblueth E (1964). Espectros de temblores a distancias moderadas y grandes. *Boletin Sociedad Mexicana de Ingenieria Sesmica*, **2** 1–18

[2] Johnson RA (1973). An earthquake spectrum prediction technique. *Bulletin of the Seismological Society of America*, **63** (4), 1255–1274

[3] Power M, Chiou BJ, Abrahamson N, Bozorgnia Y, Shantz T, Roblee C (2008). An Overview of the NGA Project. *Earthquake Spectra*, **24** (1), 3–21

[4] Chiou BJ, Darragh R, Gregor N, Silva W (2008). NGA Project Strong-Motion Database. *Earthquake Spectra*, **24** (1), 23–44

[5] Abrahamson N, Silva W (2008). Summary of the Abrahamson & Silva NGA ground-motion relations. *Earthquake Spectra*, **24** (1), 67–97

[6]   Boore DM, Atkinson GM (2008). Ground-Motion Prediction Equations for the Average Horizontal Component of PGA, PGV, and 5%-Damped PSA at Spectral Periods between 0.01 *s* and 10.0 *s*. *Earthquake Spectra*, **24** (1), 99–138

[7]   Campbell KW, Bozorgnia Y (2008). NGA Ground Motion Model for the Geometric Mean Horizontal Component of PGA, PGV, PGD and 5% Damped Linear Elastic Response Spectra for Periods Ranging from 0.01 to 10 *s*. *Earthquake Spectra*, **24** (1), 139–171

[8]   Chiou BJ, Youngs RR (2008). An NGA Model for the Average Horizontal Component of Peak Ground Motion and Response Spectra. *Earthquake Spectra*, **24** (1), 173–215

[9]   Idriss IM (2008). An NGA Empirical Model for Estimating the Horizontal Spectral Values Generated By Shallow Crustal Earthquakes. *Earthquake Spectra*, **24** (1), 217–242

[10]   Bozorgnia Y, Abrahamson N , Atik LA, Ancheta TD, Atkinson GM, Baker JW, Baltay A, Boore DM, Campbell KW, Chiou BS-J, Darragh R, Day S, Donahue J, Graves RW, Gregor N, Hanks T, Idriss IM, Kamai R, Kishida T, Kottke A, Mahin SA, Rezaeian S, Rowshandel B, Seyhan E, Shahi S, Shantz T, Silva W, Spudich P, Stewart JP, Watson-Lamprey J, Wooddell K, Youngs R (2014). NGA-West2 Research Project. *Earthquake Spectra*, **30** (3), 973–987

[11]   Ancheta TD, Darragh RB, Stewart JP, Seyhan E, Silva WJ, Chiou BS-J, Wooddell KE, Graves RW, Kottke AR, Boore DM, Kishida T, Donahue JL (2014). NGA-West2 Database. *Earthquake Spectra*, **30** (3), 989–1005

[12]   Abrahamson NA, Silva WJ, Kamai R (2014). Summary of the ASK14 Ground Motion Relation for Active Crustal Regions. *Earthquake Spectra*, **30** (3), 1025–1055

[13]   Boore DM, Stewart JP, Seyhan E, Atkinson GM (2014). NGA-West2 Equations for Predicting PGA, PGV, and 5% Damped PSA for Shallow Crustal Earthquakes. *Earthquake Spectra*, **30** (3), 1057–1085

[14]   Campbell KW, Bozorgnia Y (2014). NGA-West2 Ground Motion Model for the Average Horizontal Components of PGA, PGV, and 5% Damped Linear Acceleration Response Spectra. *Earthquake Spectra*, **30** (3), 1087–1115

[15]   Chiou BS-J, Youngs RR (2014). Update of the Chiou and Youngs NGA Model for the Average Horizontal Component of Peak Ground Motion and Response Spectra. *Earthquake Spectra*, **30** (3), 1117–1153

[16]   Idriss IM (2014). An NGA-West2 Empirical Model for Estimating the Horizontal Spectral Values Generated by Shallow Crustal Earthquakes. *Earthquake Spectra*, **30** (3), 1155–1177

[17]   Boore DM, Atkinson GM (2008). Ground-Motion Prediction Equations for the Average Horizontal Component of PGA, PGV, and 5%-Damped PSA at Spectral Periods between 0.01 *s* and 10.0 *s*. *Earthquake Spectra*, **24** (1), 99–138

[18]   Chiou B, Youngs R, Abrahamson N, Addo K (2010). Ground-Motion Attenuation Model for Small-To-Moderate Shallow Crustal Earthquakes in California and Its Implications on Regionalization of Ground-Motion Prediction Models. *Earthquake Spectra*, **26** (4), 907–926

[19]   Atkinson GM, Adams J (2013). Ground motion prediction equations for application to the 2015 Canadian national seismic hazard maps. *Canadian Journal of Civil Engineering*, **40** (10), 988–998

[20]   Atkinson GM, Boore DM (2006). Earthquake Ground-Motion Prediction Equations for Eastern North America. *Bulletin of the Seismological Society of America*, **96** (6), 2181–2205

[21]   Pezeshk S, Zandieh A, Tavakoli B (2011). Hybrid Empirical Ground-Motion Prediction Equations for Eastern North America Using NGA Models and Updated Seismological Parameters. *Bulletin of the Seismological Society of America*, **101** (4), 1859–1870

[22]   Akkar S, Bommer JJ (2010). Empirical Equations for the Prediction of PGA, PGV, and Spectral Accelerations in Europe, the Mediterranean Region, and the Middle East. *Seismological Research Letters*, **81** (2), 195–206

[23]   Akkar S, Bommer JJ (2007). Empirical Prediction Equations for Peak Ground Velocity Derived from Strong-Motion Records from Europe and the Middle East. *Bulletin of the Seismological Society of America*, **97** (2), 511–530

8

[24] Scasserra G, Stewart JP, Bazzurro P, Lanzo G, Mollaioli F (2009). A Comparison of NGA Ground-Motion Prediction Equations to Italian Data. *Bulletin of the Seismological Society of America*, **99** (5), 2961–2978

[25] Bindi D, Luzi L, Massa M, Pacor F (2010). Horizontal and vertical ground motion prediction equations derived from the Italian Accelerometric Archive (ITACA). *Bulletin of Earthquake Engineering*, **8** (5), 1209–1230

[26] Zhao JX, Zhang J, Asano A, Ohno Y, Oouchi T, Takahashi T, Ogawa H, Irikura K, Thio HK, Somerville PG, Fukushima Y, Fukushima Y (2006). Attenuation Relations of Strong Ground Motion in Japan Using Site Classification Based on Predominant Period. *Bulletin of the Seismological Society of America*, **96** (3), 898–913

[27] Kanno T, Narita A, Morikawa N, Fujiwara H, Fukushima Y (2006). A New Attenuation Relation for Strong Ground Motion in Japan Based on Recorded Data. *Bulletin of the Seismological Society of America*, **96** (3), 879–897

[28]   Bradley BA (2013). A New Zealand-Specific Pseudospectral Acceleration Ground-Motion Prediction Equation for Active Shallow Crustal Earthquakes Based on Foreign Models. *Bulletin of the Seismological Society of America*, **103** (3), 1801–1822

[29] Li X, Zhai C, Wen W, Xie L (2018). Ground Motion Prediction Model for Horizontal PGA, 5% Damped Response Spectrum in Sichuan-Yunnan Region of China. *Journal of Earthquake Engineering*, 1–38

[30] Wang D, Xie L, Abrahamson NA, Li S (2010). Comparison of Strong Ground Motion from the Wenchuan, China, Earthquake of 12 May 2008 with the Next Generation Attenuation (NGA) Ground-Motion Models. *Bulletin of the Seismological Society of America*, **100** (5B), 2381–2395

[31] Douglas J (2003). Earthquake ground motion estimation using strong-motion records: a review of equations for the estimation of peak ground acceleration and response spectral ordinates. *Earth-Science Reviews*, **61** (1–2), 43–104

[32] Adeli H (2001). Neural Networks in Civil Engineering: 1989–2000. *Computer-Aided Civil and Infrastructure Engineering*, **16** (2), 126–142

[33] Adeli H, Hung S (1995). *Machine Learning: Neural Networks, Genetic Algorithms, and Fuzzy Systems*

[34] Adeli H, Panakkat A (2009). A probabilistic neural network for earthquake magnitude prediction. *Neural Networks*, **22** (7), 1018–1024

[35] Adeli H, Wu M (1998). Regularization Neural Network for Construction Cost Estimation. *Journal of Construction Engineering and Management*, **124** (1), 18–24

[36] Derras B, Bard P-Y, Cotton F, Bekkouche A (2012). Adapting the Neural Network Approach to PGA Prediction: An Example Based on the KiK-net Data. *Bulletin of the Seismological Society of America*, **102** (4), 1446–1461

[37] Derras B, Bard P-Y, Cotton F (2016). Site-Condition Proxies, Ground Motion Variability, and Data-Driven GMPEs: Insights from the NGA-West2 and RESORCE Data Sets. *Earthquake Spectra*, **32** (4), 2027–2056

[38] Kim T, Kwon O-S, Song J (2019). Response prediction of nonlinear hysteretic systems by deep neural networks. *Neural Networks*, **111** 1–10

[39] Kong Q, Trugman DT, Ross ZE, Bianco MJ, Meade BJ, Gerstoft P (2019). Machine Learning in Seismology: Turning Data into Insights. *Seismological Research Letters*, **90** (1), 3–14

[40] Perez-Ramirez CA, Amezquita-Sanchez JP, Valtierra-Rodriguez M, Adeli H, Dominguez-Gonzalez A, Romero-Troncoso RJ (2019). Recurrent neural network model with Bayesian training and mutual information for response prediction of large buildings. *Engineering Structures*, **178** 603–615

[41] Acharya U, ROh SL, Hagiwara Y, Tan JH, Adeli H, Subha DP (2018). Automated EEG-based screening of depression using deep convolutional neural network. *Computer Methods and Programs in Biomedicine*, **161** 103–113

[42] Rafiei MH, Adeli H (2018). A novel unsupervised deep learning model for global and local health condition assessment of structures. *Engineering Structures*, **156** 598–607

[43] Schmidhuber J (2015). Deep Learning in neural networks: An overview. *Neural Networks*, **61** 85–117

9

[44]   LeCun Y, Bengio Y, Hinton G (2015). Deep learning. *Nature*, **521** (7553), 436–444

[45]   Nguyen T, Kashani A, Ngo T, Bordas S (2019). Deep neural network with high-order neuron for the prediction of foamed concrete strength. *Computer-Aided Civil and Infrastructure Engineering*, **34** (4), 316–332

[46]   Boore DM (2010). Orientation-Independent, Nongeometric-Mean Measures of Seismic Intensity from Two Horizontal Components of Motion. *Bulletin of the Seismological Society of America*, **100** (4), 1830–1835

[47]   Abrahamson NA, Youngs RR (1992). A stable algorithm for regression analyses using the random effects model. *Bulletin of the Seismological Society of America*, **82** (1), 505–510